

Supplementary information

High-performance Gas Sensor Array for Indoor Air Quality Monitoring: The Role of Au Nanoparticles in WO_3 , SnO_2 , and NiO -based Gas Sensors

Jinho Lee^{a‡}, Youngmo Jung^{b‡}, Seunghyeon Seong^b, Gil-Ho Lee^b, Jungmo Kim^a, Seong Jin^b, Young-Seok Shim^{*c}, Seong Chan Jeon^{*b}, Seokwoo Jeon^{*a}

^aDepartment of Materials Science and Engineering, Korea Advanced Institute of Science and Technology (KAIST), Daejeon 34141, Republic of Korea. E-mail: jeon39@kaist.ac.kr.

^bSchool of Mechanical Engineering, Yonsei University, 50 Yonsei-ro, Seodaemun-gu, Seoul 03722, South Korea. E-mail: scj@yonsei.ac.kr

^cDivision of Materials Science & Engineering, Silla University, 140 Baegyang-daero 700beon-gil, Sasang-gu, Busan, Republic of Korea. E-mail: ysshim@silla.ac.kr

‡ These authors contributed equally

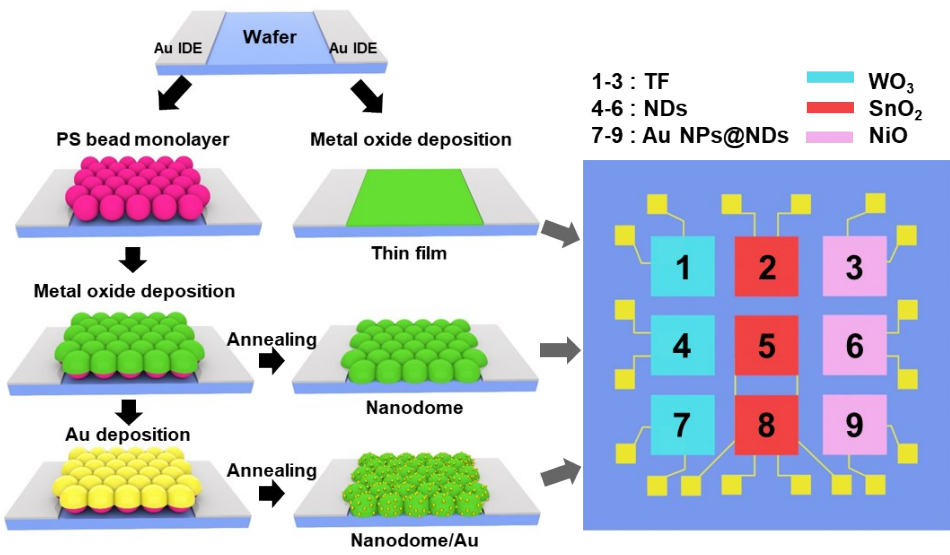


Fig. S1 Fabrication process of 3x3 gas sensor array

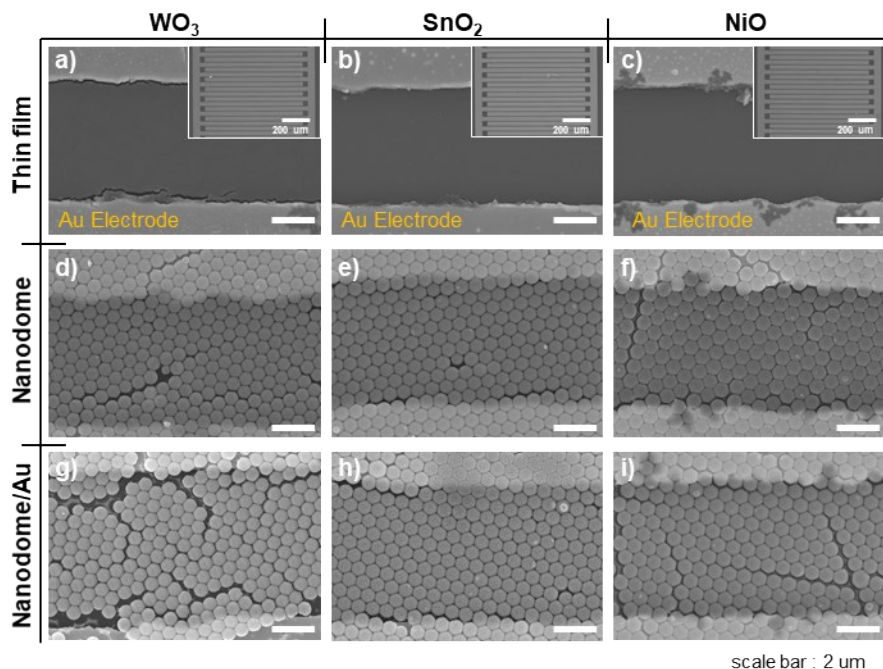


Fig. S2 SEM micrographs of the a-c) TF, d-f) NDs, g-i) Au NPs@ WO_3 , SnO_2 and NiO NDs.
The inset image show the whole IDE substrate.

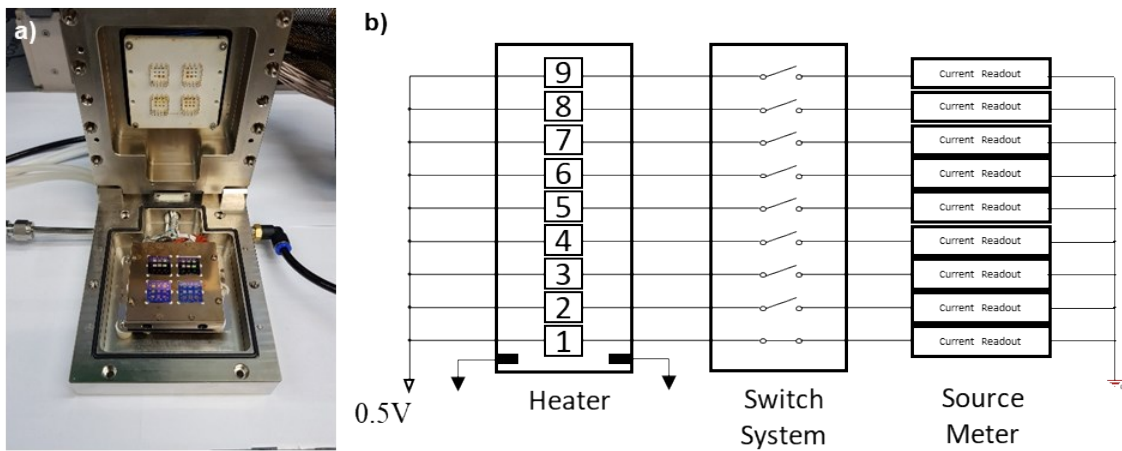


Fig. S3 a) Digital image of the gas response measurement setup and the b) interface circuitry for the gas sensing measurements of the 3x3 sensor array.

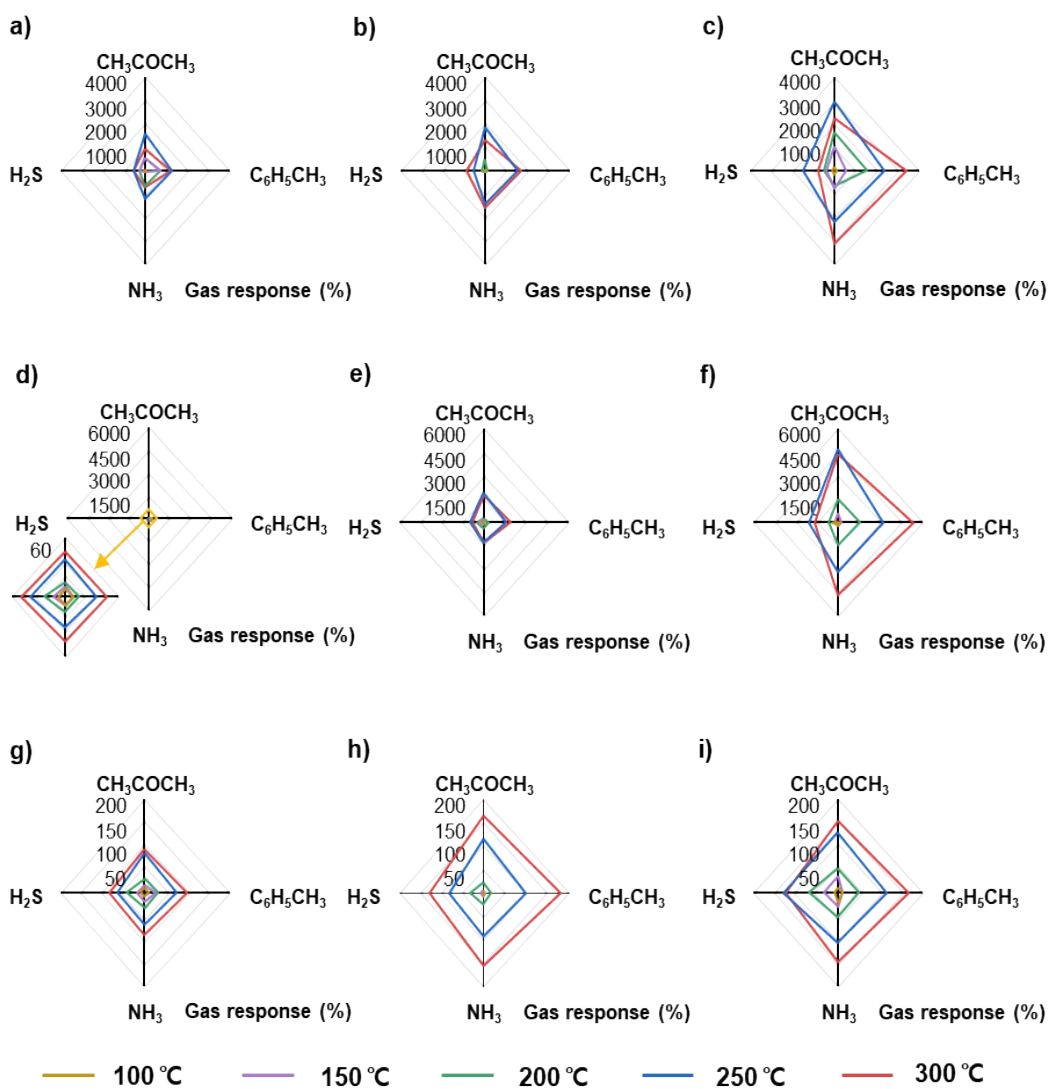


Fig. S4 Polar plot of gas responses for a-c) WO_3 , d-f) SnO_2 , g-i) NiO TFs, NDs, and Au NPs@NDs as a function of temperature.

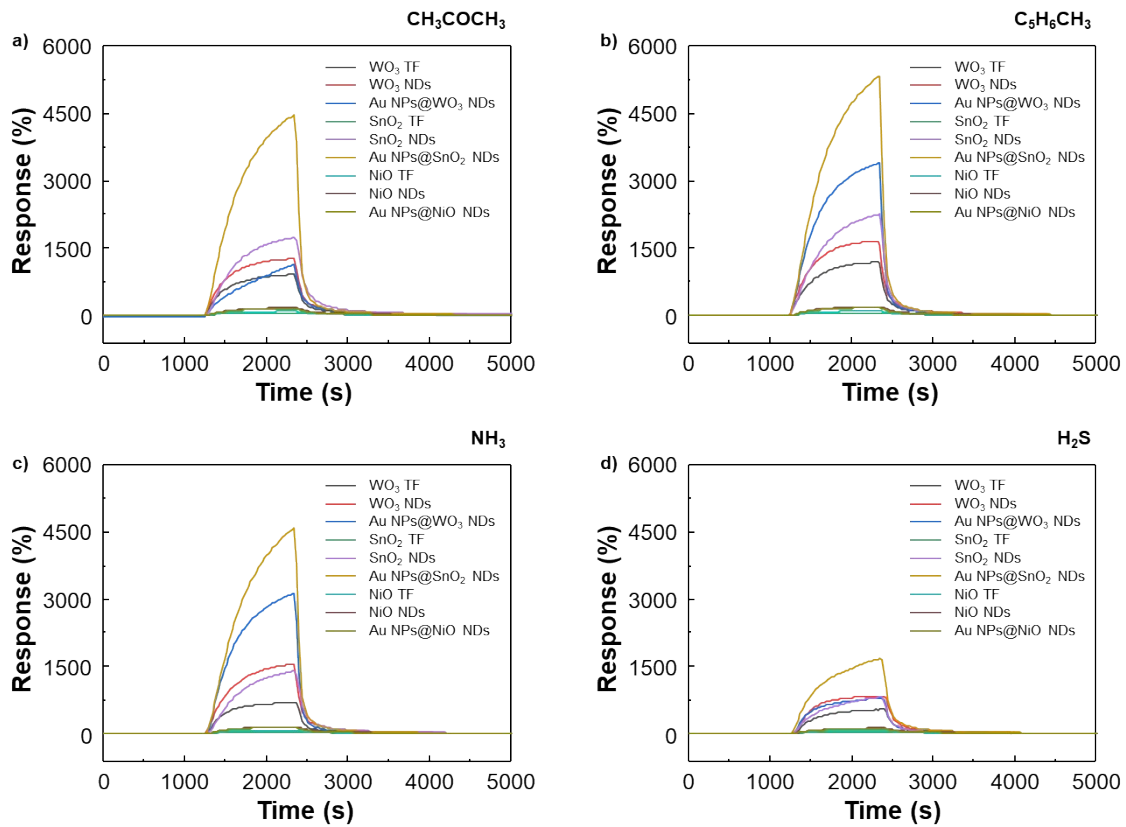


Fig. S5 Real-time response of the sensor array to 10 ppm a) CH₃COCH₃, b) C₆H₅CH₃, c) NH₃ and d) H₂S at 300 °C.

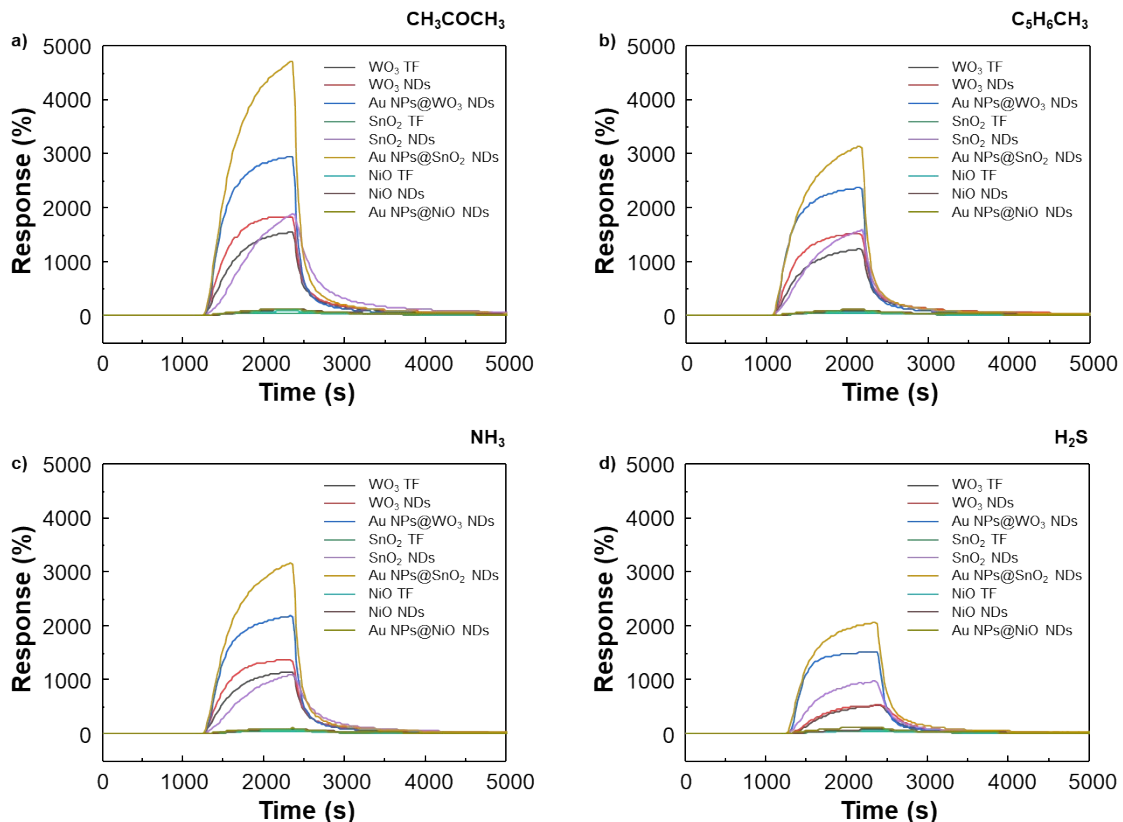


Fig. S6 Real-time response of the sensor array to 10 ppm a) CH₃COCH₃, b) C₆H₅CH₃, c) NH₃ and d) H₂S at 250 °C.

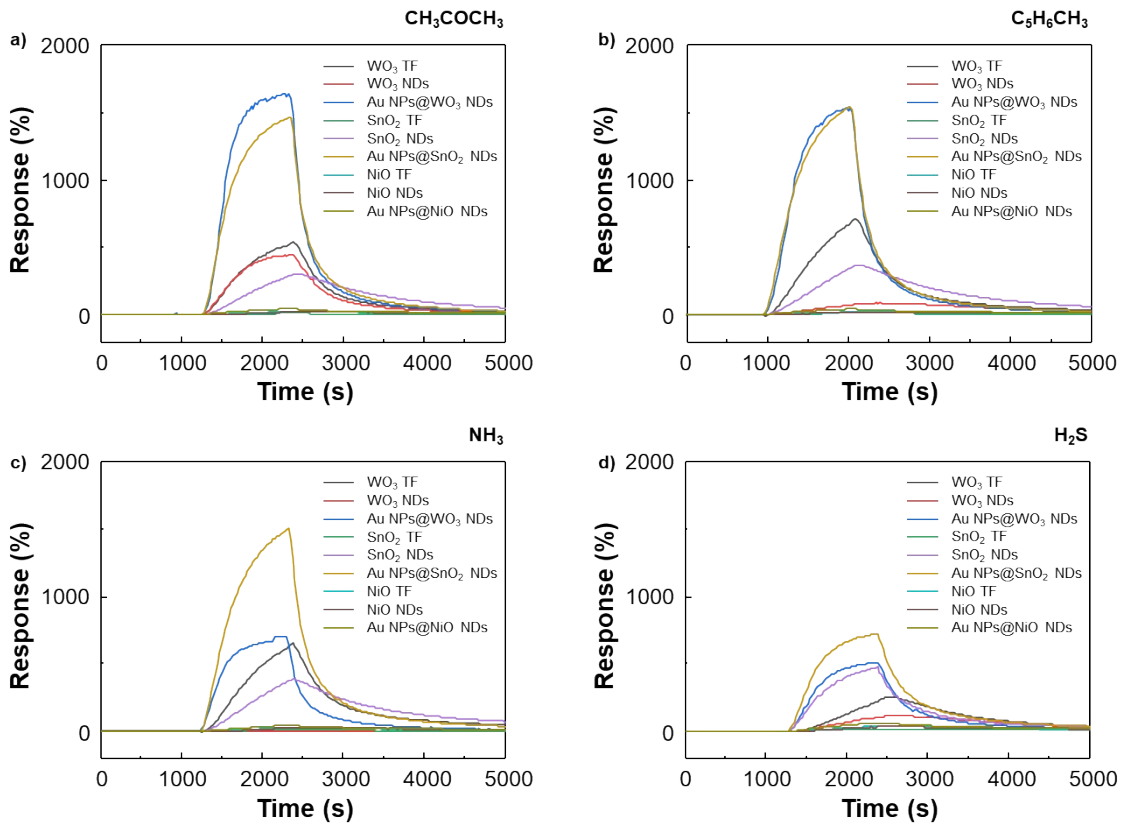


Fig. S7 Real-time response of the sensor array to 10 ppm a) CH_3COCH_3 , b) $\text{C}_6\text{H}_5\text{CH}_3$, c) NH_3 and d) H_2S at 200 °C.

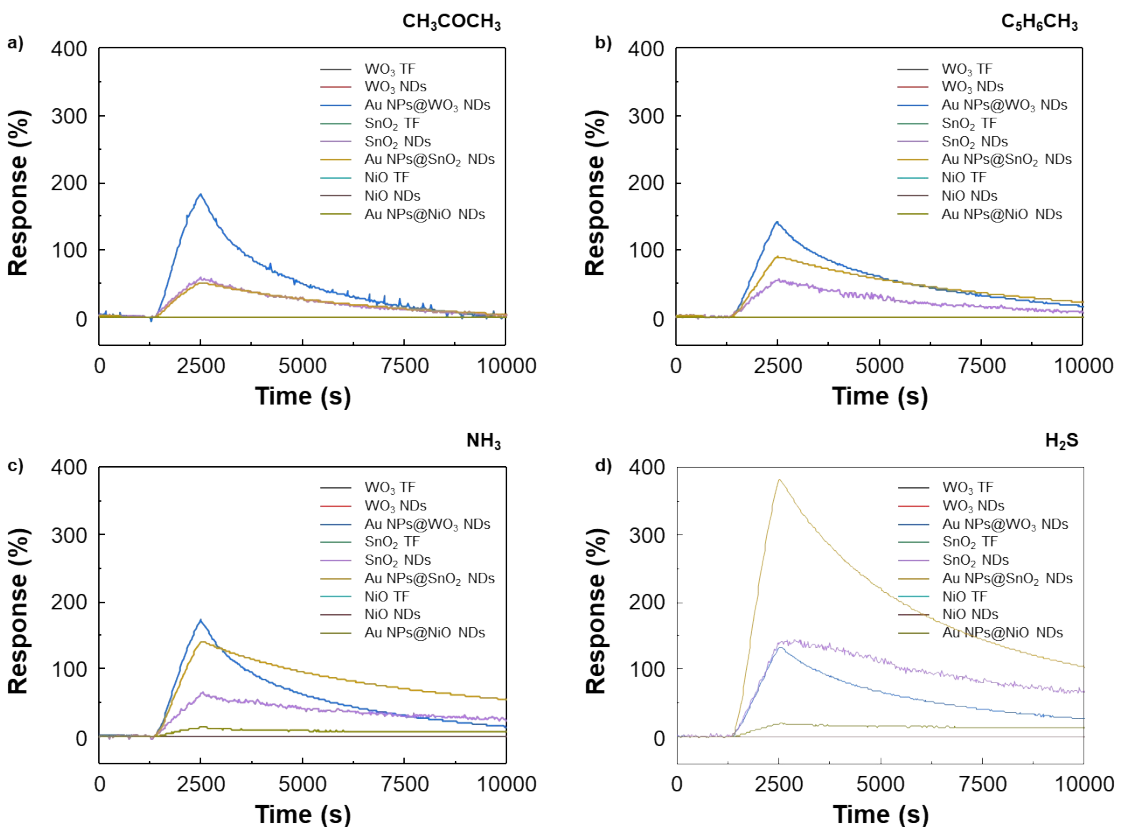


Fig. S8 Real-time response of the sensor array to 10 ppm a) CH_3COCH_3 , b) $\text{C}_6\text{H}_5\text{CH}_3$, c) NH_3 and d) H_2S at 150 °C.

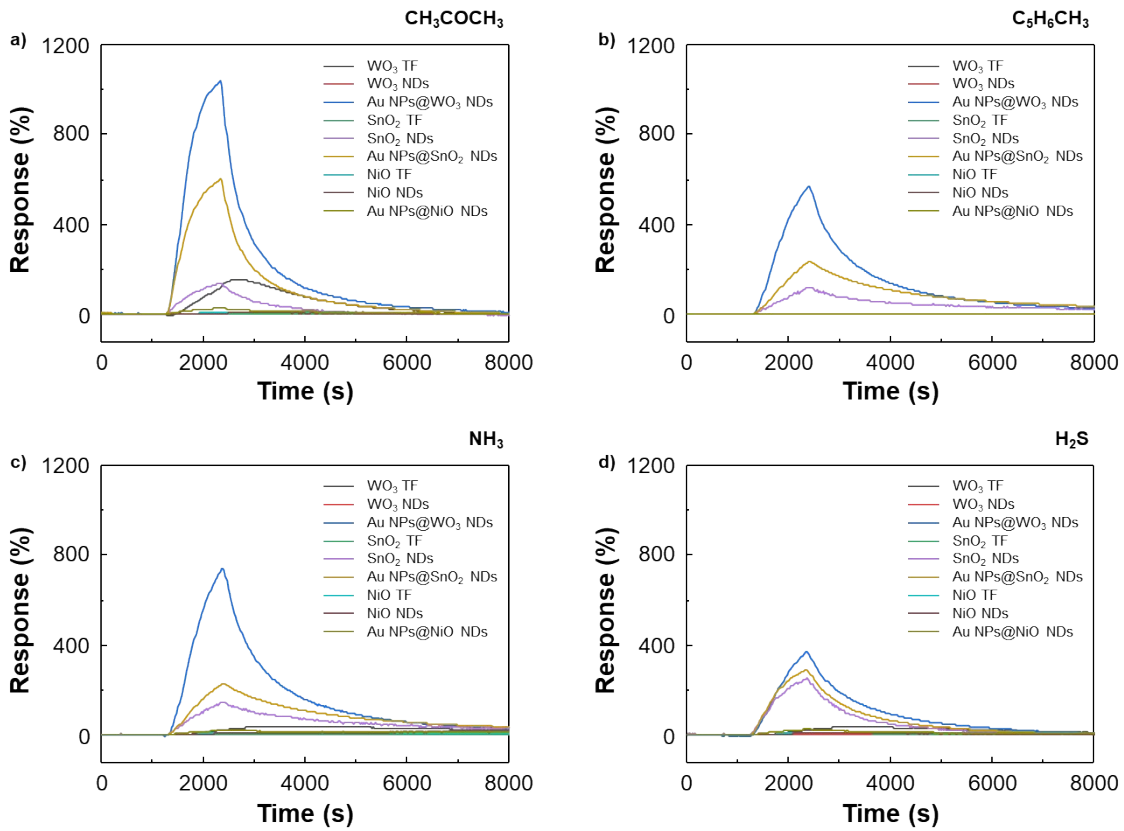


Fig. S9 Real-time response of the sensor array to 10 ppm a) CH_3COCH_3 , b) $\text{C}_6\text{H}_5\text{CH}_3$, c) NH_3 and d) H_2S at 100 °C

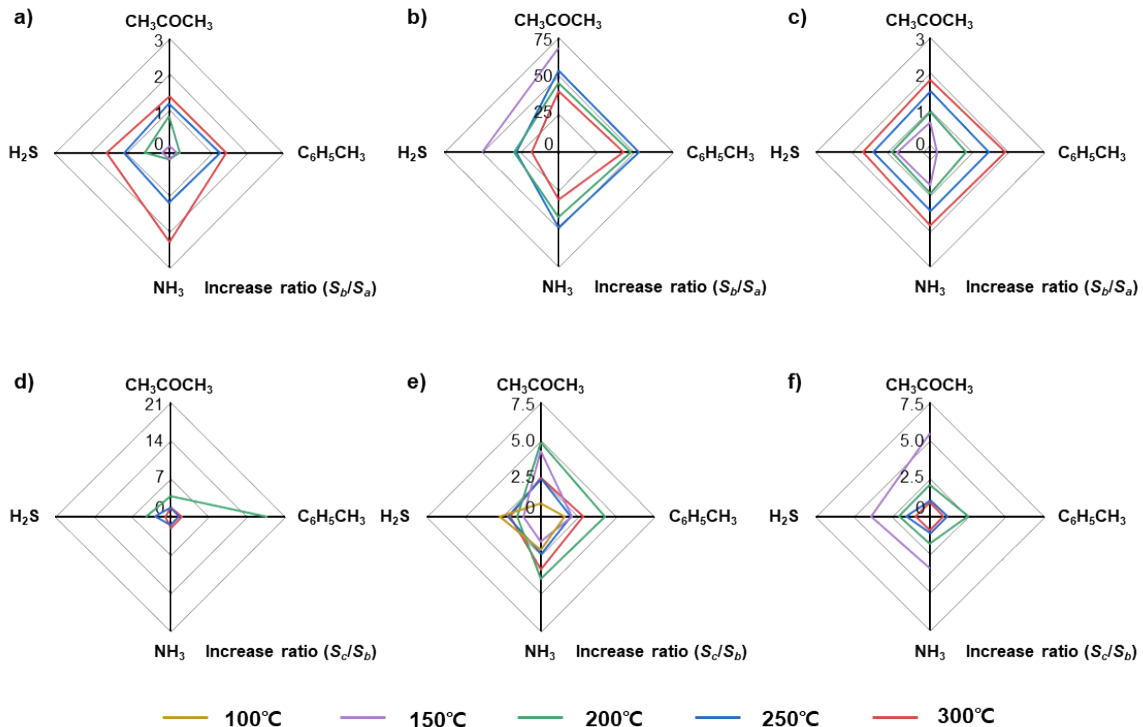


Fig. S10 Polar plots of the increase ratio (S_b/S_a) between the response of TFs and the NDs of a) WO_3 , b) SnO_2 , and c) NiO . Polar plots of the increase ratio (S_c/S_b) between the response of NDs and the Au NPs@NDs of d) WO_3 , and e) SnO_2 , f) NiO . S_a , S_b and S_c represent the responses of the TFs and NDs and Au NPs@NDs.

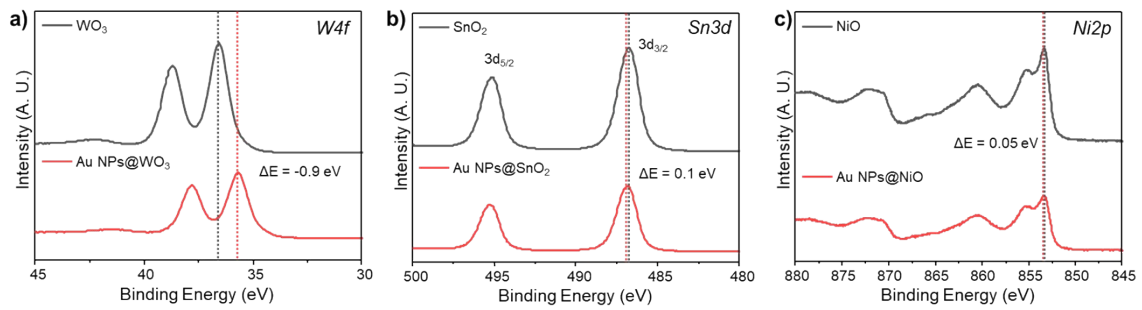


Fig. S11 XPS spectra for a) W4f of WO_3 and $\text{Au NPs}@{\text{WO}_3}$, b) Sn3d of SnO_2 and $\text{Au NPs}@{\text{SnO}_2}$ c) Ni2p of NiO and $\text{Au NPs}@{\text{NiO}}$.

Gas	Metal oxide	Type	Resistance (Ω)				
			Temperature (°C)				
			100	150	200	250	300
CH_3COCH_3	WO_3	TF	-	2.62×10^7	2.05×10^7	1.64×10^7	4.60×10^6
		NDs	-	-	9.07×10^7	7.92×10^7	2.48×10^7
		Au NPs@NDs	5.86×10^7	6.23×10^7	5.29×10^7	4.40×10^7	1.04×10^7
	SnO_2	TF	-	3.49×10^2	3.71×10^2	4.76×10^2	4.70×10^2
		NDs	2.45×10^6	3.18×10^6	1.69×10^4	6.90×10^4	5.10×10^4
		Au NPs@NDs	1.62×10^3	2.33×10^4	7.42×10^4	2.19×10^5	1.96×10^5
	NiO	TF	-	6.70×10^5	9.43×10^4	2.00×10^4	7.39×10^3
		NDs	-	2.94×10^7	4.57×10^6	6.33×10^5	1.63×10^5
		Au NPs@NDs	-	1.20×10^7	1.36×10^6	2.15×10^5	6.11×10^4
$\text{C}_6\text{H}_5\text{CH}_3$	WO_3	TF	-	-	4.25×10^7	1.28×10^7	5.26×10^6
		NDs	-	-	4.09×10^6	6.48×10^7	2.73×10^7
		Au NPs@NDs	8.05×10^7	6.16×10^7	5.38×10^7	3.20×10^7	2.47×10^7
	SnO_2	TF	-	-	3.88×10^2	4.51×10^2	4.66×10^2
		NDs	5.49×10^6	8.20×10^6	3.68×10^4	2.33×10^5	2.98×10^5
		Au NPs@NDs	3.06×10^3	5.05×10^3	8.42×10^4	1.41×10^5	2.26×10^5
	NiO	TF	-	6.42×10^6	8.26×10^4	2.34×10^4	7.73×10^3
		NDs	-	-	3.78×10^6	7.69×10^5	1.69×10^5
		Au NPs@NDs	8.29×10^7	-	1.21×10^6	2.46×10^5	6.42×10^4
NH_3	WO_3	TF	-	7.50×10^6	8.82×10^6	5.00×10^6	2.15×10^6
		NDs	-	-	3.39×10^6	2.56×10^6	1.42×10^6
		Au NPs@NDs	2.15×10^7	2.15×10^7	8.88×10^6	4.56×10^6	2.03×10^6
	SnO_2	TF	-	-	3.86×10^2	4.36×10^2	4.72×10^2
		NDs	3.87×10^6	5.79×10^6	2.41×10^4	5.02×10^4	6.15×10^4
		Au NPs@NDs	3.06×10^3	4.44×10^3	7.30×10^4	1.75×10^5	2.59×10^5
	NiO	TF	-	3.88×10^5	1.06×10^5	2.32×10^4	7.69×10^3
		NDs	-	1.62×10^7	8.93×10^6	7.89×10^5	1.65×10^5
		Au NPs@NDs	8.08×10^7	5.39×10^6	1.41×10^6	2.55×10^5	6.48×10^4
H_2S	WO_3	TF	-	4.76×10^7	3.57×10^7	1.96×10^7	8.54×10^6
		NDs	-	-	1.20×10^7	9.53×10^6	6.23×10^6
		Au NPs@NDs	4.29×10^7	3.43×10^7	1.35×10^7	6.67×10^6	3.05×10^6
	SnO_2	TF	-	4.14×10^2	4.48×10^2	5.27×10^2	5.20×10^2
		NDs	1.40×10^7	8.91×10^6	1.03×10^7	1.53×10^7	9.26×10^6
		Au NPs@NDs	9.60×10^3	5.74×10^3	9.38×10^3	1.88×10^4	1.51×10^4
	NiO	TF	-	5.18×10^5	8.51×10^4	2.02×10^4	8.32×10^3
		NDs	-	1.97×10^7	3.00×10^6	5.48×10^5	1.67×10^5
		Au NPs@NDs	3.13×10^7	6.61×10^6	9.60×10^5	1.94×10^5	6.57×10^4

Table S1 Resistance of each sensors with operating temperature.

$\Delta (E_{TF} - E_{NDs})$ (kJ/mol)	WO ₃	SnO ₂	NiO
CH ₃ COCH ₃	-15.9	4.67	-14.8
C ₆ H ₅ CH ₃	-46.3	0.902	-28.9
NH ₃	-14.2	-1.92	-13.2
H ₂ S	10.0	6.22	-12.1

Table S2 Difference in the activation energy between TF and NDs ($E_{TF} - E_{NDs}$) of each metal oxide and gas combination.